Van der Waals theory of nematogenic solutions. II. Application to binary solutions with spherical solutes and rodlike solvents

Martha A. Cotter and Douglas C. Wacker

Department of Chemistry, Rutgers, The State University, New Brunswick, New Jersey 08903
(Received 27 June 1978)

The Van der Waals theory of nematogenic solutions derived in Paper I of this series is here applied to binary mixtures with effectively spherical solute molecules and rodlike solvent molecules. Predicted temperature–mole-fraction phase diagrams are shown to be in rather good agreement with experimental data for the systems CCl_4-p,p'-dihexyloxyazoxybenzene (DHAB), $(CH_3)_4$Sn-methoxybenzylidene n-butylaniline (MBBA), $(C_2H_5)_4$Sn-MBBA, $(C_3H_7)_4$Sn-MBBA, and $(C_4H_9)_4$Sn-MBBA. On the basis of these calculations, it .is argued that when a more or less spherical solute is added to a nematic mesophase, the onset of the nematic→isotropic phase transition is controlled primarily by excluded-volume effects and the overall strength of the intermolecular attractions in the system.

I. INTRODUCTION AND THEORY

In Paper I[1] of this series of papers—hereafter referred to simply as I—we presented a Van der Waals theory of nematogenic solutions, applicable to mixtures of any number of components with rodlike or effectively spherical molecular shapes. In this paper, Paper II of the series, we apply the general theory to binary solutions with effectively spherical solute molecules and rodlike solvent molecules. We have chosen to study these solutions first because they are the simplest systems to which the theory can be applied and the nematogenic solutions for which the most experimental data are available. Moreover, an understanding of the effects of adding more or less spherical solutes to nematic mesophases is of considerable practical importance, since small amounts of such materials are frequently added to the nematogenic mixtures used in liquid-crystal displays (in order to adjust the viscosity-electrical conductivity).

Our model system, then, is a binary mixture of yN spherical solute molecules and $(1-y)N$ rodlike solvent molecules in a volume V at temperature T. Each solvent molecule has a spherocylindrical hard core of radius a and cylindrical length l, while each solute molecule has a spherical hard core of radius $R_a a$. The solvent-solvent, solvent-solute, and solute-solute pair potentials are given by

$$v_{00}(\vec{r}_{ij}, \Omega_i, \Omega_j) = v_{00}^*(\vec{r}_{ij}, \Omega_i, \Omega_j)$$
$$+ v_{00}^{(a)}(\vec{r}_{ij}, \Omega_i, \Omega_j),$$

$$v_{0s}(\vec{r}_{jk}) = v_{0s}^*(\vec{r}_{jk}) + v_{0s}^{(a)}(\vec{r}_{jk}),$$

and

$$v_{ss}(r_{kl}) = v_{ss}^*(r_{kl}) + v_{ss}^{(a)}(r_{kl}),$$

respectively, where Ω_i and Ω_j denote the orientations of rodlike molecules i and j, the v^*'s are hard-core repulsions, and the $v^{(a)}$'s are somewhat longer-ranged attractions (which we shall specify later). For this system, Eqs. (22), (26), and (27) of I—which give the configurational Helmholtz free energy, the pressure, and the configurational chemical potentials, respectively, reduce to

$$\frac{F_c}{Nk_BT} = (1-y)\ln(1-y) + y\ln y + (1-y)\int d\Omega \bar{f}_0(\Omega)\ln[4\pi\bar{f}_0(\Omega)] - 1 + \ln\left(\frac{\rho}{1-\bar{v}\rho}\right) + \frac{\rho B}{2(1-\bar{v}\rho)}$$

$$+ \frac{\rho^2 C}{3(1-\bar{v}\rho)^2} + \tfrac{1}{2}\beta\left((1-y)\int d\Omega \bar{f}_0(\Omega)\bar{\psi}_0(\rho,\Omega) + y\bar{\psi}_s(\rho)\right), \tag{1}$$

$$\frac{P}{k_BT} = \frac{\rho}{1-\bar{v}\rho} + \frac{\rho^2 B}{2(1-\bar{v}\rho)^2} + \frac{2\rho^3 C}{3(1-\bar{v}\rho)^3} + \tfrac{1}{2}\beta\rho\left((1-y)\int d\Omega \bar{f}_0(\Omega)\bar{\psi}_0(\Omega,\rho) + y\bar{\psi}_s(\rho)\right), \tag{2}$$

$$\frac{\mu_{c,0}}{k_B T} = \int d\Omega \bar{f}_0(\Omega) \ln[4\pi \bar{f}_0(\Omega)] + \ln\left(\frac{(1-y)\rho}{1-\bar{v}\rho}\right) + \frac{6(1-y)v_0\rho(1+\frac{2}{3}r\Gamma) + [R_a(1+R_a)(2+q) - R_a^2(1-q)]yv_0\rho}{1-\bar{v}\rho}$$

$$+ \frac{v_0^2\rho^2\{2(1-y)^2(2+q)(1-\frac{1}{4}q+r\Gamma) + y(1-y)[(4v_s/v_0R_a)(1-\frac{1}{4}q+r\Gamma) + \frac{2}{3}R_a^2(2+q)^2] + \frac{3}{2}R_a(2+q)(v_s/v_0)y^2\}}{(1-\bar{v}\rho)^2}$$

$$+ \frac{P^*v_0}{k_B T} + \beta \int d\Omega \bar{f}_0(\Omega)\bar{\psi}_0(\Omega,\rho), \tag{3}$$

and

$$\frac{\mu_{c,s}}{k_B T} = \ln\left(\frac{y\rho}{1-\bar{v}\rho}\right) + \frac{6yv_s\rho + [R_a(1+R_a)(2+q) - R_a^2(1-q)](1-y)v_0\rho}{1-\bar{v}\rho}$$

$$+ \frac{\frac{9}{2}y^2v_s^2\rho^2 + 3R_a(2+q)y(1-y)v_0v_s\rho^2 + [(2v_0v_s/R_a)(1-\frac{1}{4}q+r\Gamma) + \frac{1}{3}v_0^2R_a^2(2+q)^2](1-y)^2\rho^2}{(1-\bar{v}\rho)^2} + \frac{P^*v_s}{k_B T} + \beta\bar{\psi}_s(\rho),$$

where ρ is the number density N/V; $\beta = 1/k_B T$; the subscripts 0 and s refer to the solvent and solute, respectively;

$$v_0 = \pi a^2 l + \tfrac{4}{3}\pi a^3, \quad v_s = \tfrac{4}{3}\pi R_a^3 a^3,$$

$$\bar{v} = (1-y)v_0 + yv_s,$$

$$q = \tfrac{4}{3}\pi a^3/v_0, \quad r = al^2/v_0,$$

$$C = v_0^2\rho^2[2(1-y)^2(1-\tfrac{1}{4}q+r\Gamma) + y(1-y)R_a^2(2+q)$$

$$+ \tfrac{3}{2}y^2v_s/v_0][(1-y)(2+q)v_0\rho + 3yv_s\rho/R_a],$$

$$\Gamma = \langle\langle\,|\sin\gamma\,|\,\rangle\rangle$$

$$= \int f_0(\Omega)f_0(\Omega')\,|\sin\gamma(\Omega,\Omega')|\,d\Omega\,d\Omega',$$

$$B = 2v_0^2\rho^2\{3(1-y)^2(1+\tfrac{2}{3}r\Gamma)$$

$$+ y(1-y)[R_a(1+R_a)(2+q) - R_a^2(1-q)]$$

$$+ 3y^2v_s/v_0\},$$

$$\bar{\psi}_0(\rho,\Omega) = \rho\left((1-y)\int \bar{f}_0(\Omega')\,d\Omega'\int d\bar{r}\;\exp[-\beta v_{00}^*(\bar{r},\Omega,\Omega^1)]v_{00}^{(a)}(\bar{r},\Omega,\Omega') + y\int d\bar{r}\exp[-\beta v_{0s}^*(\bar{r})]v_{0s}^{(a)}(\bar{r})\right) \tag{5}$$

$$\equiv \rho[(1-y)I_{00}(\Omega) + yI_{ss}],$$

$$\bar{\psi}_s(\rho) = \rho\left((1-y)\int d\bar{r}\exp[-\beta v_{0s}^*(\bar{r})]v_{0s}^{(a)}(\bar{r}) + y\int d\bar{r}\exp[-\beta v_{ss}^*(r)]v_{ss}^{(a)}(r)\right) \tag{6}$$

$$\equiv \rho[(1-y)I_{0s} + yI_{ss}];$$

$P^*/k_B T$ represents the first three terms on the right-hand side of (2); and $\gamma(\Omega,\Omega')$ is the angle between directions Ω and Ω'. v_0 and v_s are clearly the solvent and solute molecular volumes and $\bar{\psi}_0$ and $\bar{\psi}_s$ are the pseudopotentials describing the interaction of a solvent or solute molecule, respectively, with the mean field resulting from attractions between it and its neighbors. $\bar{f}_0(\Omega)$, the equilibrium single-particle orientational distribution function for the solvent, can be obtained by solving the integral equation

$$0 = \omega + \ln[4\pi\bar{f}_0(\Omega)] + \beta(1-y)\rho I_{00}(\Omega)$$

$$+ \frac{4r(1-y)v_0\rho}{1-\bar{v}\rho}\left(1 + \frac{(2+q)(1-y)v_0\rho + 3yR_a^{-1}v_s\rho}{3(1-\bar{v}\rho)}\right)$$

$$\times \int \bar{f}_0(\Omega')\,|\sin\gamma(\Omega,\Omega')|\,d\Omega' \tag{7}$$

derived by minimizing the functional $N^{-1}F_c[f_0(\Omega)]$. The constant ω appearing in (7) can be evaluated using the normalization constraint

$$\int \bar{f}_0(\Omega)\,d\Omega = 1. \tag{8}$$

Before proceeding to use (1)–(8), we introduce three simplifying assumptions or approximations.

(i) We let $v_{00}^{(a)}$, $v_{0s}^{(a)}$, and $v_{ss}^{(a)}$ all be of the form

$$v_{\sigma\sigma'}^{(a)} = -\epsilon_{\sigma\sigma'}/r^6, \tag{9}$$

where r is the distance between the centers of the pair of molecules and the ϵ's are positive constants. This should be a realistic assumption for $v_{ss}^{(a)}$ and a satisfactory approximation for $v_{0s}^{(a)}$— given that one integrates over the orientation of $\bar{r}$ (relative to Ω) in evaluating I_{0s}. On the other hand, taking the attractions between rodlike solvent molecules to be orientation-independent is

clearly not very realistic. In the Van der Waals approach, however, $v_{00}^{(a)}$ contributes to the thermodynamic behavior of the system only through the integral I_{00}; and recent calculations of this quantity by Gelbart and Gelbart[2] strongly suggest that the orientation dependence of I_{00} is determined in very large part by the leading term in $v_{00}^{(a)}$, which is independent of molecular orientations.

(ii) We approximate I_{00} by

$$I_{00}(\Omega) = -\mathbf{v}_{i00} - \mathbf{v}_{a00}\eta P_2(\cos\theta) , \qquad (10)$$

where θ is the angle between the long axis of a solvent molecule and the nematic director (i.e., the "preferred" direction for molecular long axes) and

$$\eta_0 = \int \tilde{f}_0(\Omega)P_2(\cos\theta)\,d\Omega$$

$$= \int \tilde{f}_0(\Omega)[\tfrac{3}{2}\cos^2\theta - \tfrac{1}{2}]\,d\Omega. \qquad (11)$$

(10) is obtained by expanding the inner integral in I_{00} [see Eq. (5)] in even-order Legendre polynomials $P_n[\cos\gamma(\Omega,\Omega')]$, integrating over Ω' term by term, and truncating the resulting series for I_{00} after the term proportional to $P_2(\cos\theta)$. Our justification for doing this can be found in the previously cited work of Gelbart and Gelbart,[2] who showed that for molecules having spherocylindrical hard cores with length-to-width ratios between 1 and 4.2 and $v^{(a)} \propto r^{-6}$, I_{00} is approximated quite satisfactorily by (10), where, using our notation,

$$\mathbf{v}_{i00} = -\int I_{00}(\Omega)\,d\Omega , \qquad (12)$$

$$\mathbf{v}_{a00} = -\int I_{00}(\Omega)P_2(\cos\theta)\,d\Omega .$$

(iii) We approximate the quantity Γ or $\langle\langle|\sin\gamma|\rangle\rangle$ by

$$\Gamma = \langle\langle|\sin\gamma(\Omega,\Omega')|\rangle\rangle = \tfrac{1}{4}\pi(1 - \tfrac{5}{8}\eta_0^2) \qquad (13)$$

which is equivalent to expanding $|\sin\gamma(\Omega,\Omega')|$ in Legendre polynomials $P_n(\cos\gamma)$, averaging term by term, and then truncating the resulting series after its second nonvanishing term. This approximation enormously simplifies subsequent numerical computations by allowing us to derive a closed-form expression for $\tilde{f}_0(\Omega)$. It has been tested[3] for one-component systems of *hard* spherocylinders; in such cases, its introduction lowers the predicted values of the order parameter η by roughly 0.10 to 0.15 but has very little effect on any other thermodynamic quantity. One would certainly not expect the use of (13) to change the phase diagrams of our model solutions to any significant extent.

When (10) and (13) are substitued in (1) and

$N^{-1}F_c[f_0(\Omega)]$ minimized subject to the constraint (8), the resulting equation for $\tilde{f}_0(\Omega)$, replacing (7), is

$$\tilde{f}_0 = \frac{\exp[\Lambda\eta_0 P_2(\cos\theta)]}{\int d\Omega \exp[\Lambda\eta_0 P_2(\cos\theta)]} , \qquad (14)$$

where

$$\Lambda = \frac{5\pi r(1-y)v_0\rho}{8(1-\overline{v}\rho)}\left(1 + \frac{(2+q)(1-y)v_0\rho + 3yR_a^{-1}v_s\rho}{3(1-\overline{v}\rho)}\right)$$

$$+ (1-y)\rho\frac{\mathbf{v}_{a00}}{k_B} \qquad (15)$$

and the solvent order parameter η_0 is calculated (iteratively) using the consistency condition

$$\eta_0 = \int \tilde{f}_0(\Omega)P_2(\cos\theta)\,d\Omega$$

$$\times \frac{\int_0^{\pi/2}\exp[\Lambda\eta_0 P_2(\cos\theta)]P_2(\cos\theta)\sin\theta\,d\theta}{\int_0^{\pi/2}\exp[\Lambda\eta_0 P_2(\cos\theta)]\sin\theta\,d\theta} . \qquad (16)$$

Finally, to be consistent with (10), we introduce the following change in notation

$$\mathbf{v}_{i0s} \equiv -I_{0s} = -\int d\vec{\mathbf{r}}\exp[-\beta v_{0s}^*(\vec{\mathbf{r}})]v_{0s}^{(a)}(\vec{\mathbf{r}})$$

$$\mathbf{v}_{iss} \equiv -I_{ss} = -\int d\vec{\mathbf{r}}\exp[-\beta v_{ss}^*(r)]v_{ss}^{(a)}(r) \qquad (17)$$

Our equations for the pseudopotentials $\overline{\psi}_0$ and $\overline{\psi}_s$ then become

$$\overline{\psi}_0(\rho,\Omega) = -\rho\{(1-y)[\mathbf{v}_{i00} + \mathbf{v}_{a00}\eta_0 P_2(\cos\theta)] + y\mathbf{v}_{i0s}\} \qquad (18)$$

and

$$\overline{\psi}_s(\rho) = -\rho[(1-y)\mathbf{v}_{i0s} + y\mathbf{v}_{iss}] , \qquad (19)$$

while the configurational internal energy per particle is given by

$$N^{-1}E_c = \tfrac{1}{2}\rho[(1-y)^2(\mathbf{v}_{i00} + \mathbf{v}_{a00}\eta_0^2)$$

$$+ 2y(1-y)\mathbf{v}_{i0s} + y^2\mathbf{v}_{iss}] . \qquad (20)$$

The integrals $\mathbf{v}_{i0s}$ and $\mathbf{v}_{iss}$ are easily evaluated, with the results

$$\mathbf{v}_{i0s} = -\frac{4\pi\epsilon_{0s}}{3a^3(1+R_a)^3}\int_{\pi/2}^{L}\sin^4\theta\,d\theta$$

$$- \frac{4\pi\epsilon_{0s}}{3a^3}\int_0^L\frac{\sin\theta\,d\theta}{\mathcal{R}^3} \qquad (21)$$

$$\mathbf{v}_{iss} = -\tfrac{1}{6}\pi\epsilon_{ss}/(R_a a)^3 , \qquad (22)$$

where

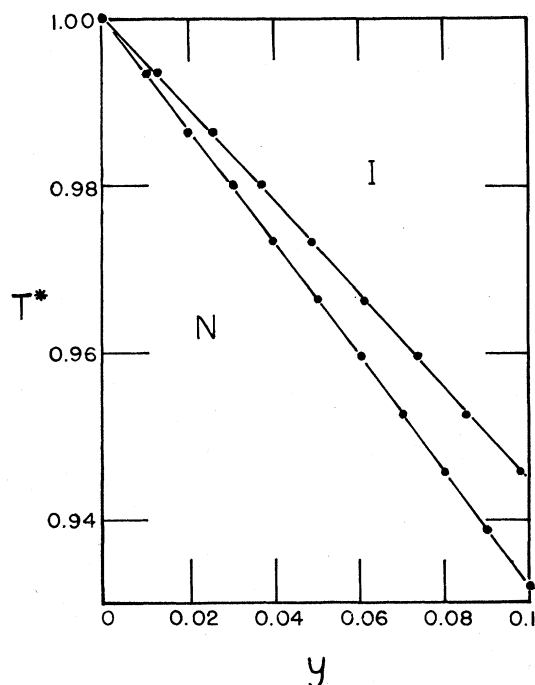$$L = \tan^{-1}[2a(1+R_a)/l] ,$$

and

FIG. 1. Calculated phase diagram for a binary mixture of hard spherocylinders and spheres. The solvent length-to-width ratio x_0 is 3.99 and $R_a = 1$. T^* is the reduced temperature $T/T_{N \to I}^0$, where $T_{N \to I}^0$ is the nematic $\to$ isotropic transition temperature for the pure solvent, and y is the solute mole fraction. The points were obtained by solving (16) and (23).

$$\mathcal{R} = (l/2a) \cos\theta + [(1 + R_a)^2 - (l/2a)^2 \sin^2\theta]^{1/2} .$$

We are now ready to use (1)–(4) and (12)–(22) to determine the thermodynamic behavior of various model nematogenic mixtures. In order to calculate the density ρ and solvent order parameter η_0 at a given T and P, it is necessary to solve (2) and (16) simultaneously. To determine the compositions and densities of coexisting nematic and isotropic phases at a particular temperature T and pressure P, one must solve the set of five simultaneous equations consisting of (16) and

$$\mu_0(T, \rho_{\text{nem}}, \eta_0) = \mu_0(T, \rho_{\text{iso}}, 0) ,$$

$$\mu_s(T, \rho_{\text{nem}}, \eta_0) = \mu_s(T, \rho_{\text{iso}}, 0) , \qquad (23)$$

$$P(T, \rho_{\text{nem}}, \eta_0) = P ,$$

$$P(T, \rho_{\text{iso}}, 0) = P .$$

II. CALCULATIONS AND RESULTS

In order to study the role of excluded volume effects in mixtures of spherical and rodlike molecules, we have considered six binary systems of hard spheres and hard spherocylinders. The solvent spherocylinders had length-to-width ratios

TABLE I. Limiting slopes, β_n^∞ and β_i^∞, of the nematic and isotropic phase boundaries for several solutions of hard spheres and hard spherocylinders. x_0 is the length-to-width ratio of the solvent spherocylinders and R_a is the ratio of the solute to the solvent radius.

x_0	R_a	β_n^∞	β_i^∞
2.93	1.0	0.784	0.623
2.93	1.5	1.674	1.080
2.93	2.0	3.195	1.558
3.99	1.0	0.648	0.529
3.99	1.5	1.279	0.887
3.99	2.0	2.290	1.278

$x_0 = (l/2a) + 1$ of either 2.93 or 3.99, and in each case solute spheres with $R_a = 1$, 1.5, and 2 were used. One of the calculated phase diagrams, that for $x_0 = 3.99$ and $R_a = 1$, is shown in Fig. 1. As can be seen, the nematic and isotropic phase boundaries are nearly linear, particularly for smaller values of y. The limiting slopes, β_n^∞ and β_i^∞, of these phase boundary lines as $y \to 0$ are given in Table I for all six systems. They were obtained using the thermodynamic relations

$$\beta_n^\infty = [1 - (\gamma_{s,n}^\infty / \gamma_{s,i}^\infty)] / (\Delta S_{N \to I}^0 / N k_B) , \qquad (24a)$$

$$\beta_i^\infty = [(\gamma_{s,i}^\infty / \gamma_{s,n}^\infty) - 1] / (\Delta S_{N \to I}^0 / N k_B) , \qquad (24b)$$

where $\Delta S_{N \to I}^0$ is the entropy change at the nematic $\to$ isotropic transition of the pure solvent and $\gamma_{s,n}^\infty$, $\gamma_{s,i}^\infty$, the infinite dilution solute activity coefficients in the nematic and isotropic phases, respectively, were evaluated using (4) and

$$\ln \gamma_s = \frac{\mu_s}{k_B T} - \frac{\mu_{s,\text{pure solute}}}{k_B T} - \ln y . \qquad (25)$$

[The limiting slopes could have been determined graphically, but (24) yields more precise results.] As can be seen from the table, the magnitude of β_n^∞ increases rapidly with increasing R_a, reflecting the increasing ability of larger solute spheres to disrupt the nematic ordering of the solvent spherocylinders. For a given R_a, moreover, the slopes are less negative when $x_0 = 3.99$ than when $x_0 = 2.93$, indicating that longer solvent rods can accommodate a higher concentration of solute spheres before the nematic order is destroyed. Although these values of β_n^∞ and β_i^∞ are significantly more negative than those observed for real systems with similar solute and solvent sizes (see below), the qualitative trends in the slopes are correct.[4]

We have also applied our theory to five nematogenic systems studied by Martire et al.[4]; namely, solutions of CCl_4 in DHAB (p,p'-dihexyloxy-azoxybenzene) and solutions of $(CH_3)_4Sn$, $(C_2H_5)_4Sn$, $(C_3H_7)_4Sn$, and $(n\text{-}C_4H_9)_4Sn$ in MBBA (methoxybenzylidene n-butylaniline). In each case, it was nec-

TABLE II. Values of the ratios R_a, $\epsilon_{ss}/\epsilon_{00}$, $\epsilon_{0s}/\epsilon_{00}$, $\mathcal{V}_{iss}/\mathcal{V}_{i00}$, and $\mathcal{V}_{i0s}/\mathcal{V}_{i00}$ used in the calculations.

System	R_a	$\dfrac{\epsilon_{ss}}{\epsilon_{00}}$	$\dfrac{\epsilon_{0s}}{\epsilon_{00}}$	$\dfrac{\mathcal{V}_{iss}}{\mathcal{V}_{i00}}$	$\dfrac{\mathcal{V}_{i0s}}{\mathcal{V}_{i00}}$
CCl_4 – DHAB	1.07	0.035	0.187	0.100	0.351
$(CH_3)_4Sn$ – MBBA	1.25	0.136	0.369	0.215	0.490
$(C_2H_5)_4Sn$ – MBBA	1.42	0.399	0.632	0.430	0.680
$(C_3H_7)_4Sn$ – MBBA	1.57	0.821	0.906	0.655	0.820
$(C_4H_9)_4Sn$ – MBBA	1.69	1.30	1.14	0.830	0.905

essary to choose a solvent hard-core radius a, a solvent length-to-width ratio x_0, a solute hard-core radius $R_a a$, and values of the constants ϵ_{00}, ϵ_{0s}, and ϵ_{ss}, from which the mean-field energy parameters $\mathcal{V}_{i00}$, $\mathcal{V}_{a00}$, $\mathcal{V}_{i0s}$, and $\mathcal{V}_{iss}$ may be obtained. For both solvents, we assumed that a = 2.5 Å, while the values of x_0 used were 3.0 for MBBA and 4.2 for DHAB. The values of R_a, $\epsilon_{0s}/\epsilon_{00}$, $\epsilon_{ss}/\epsilon_{00}$, $\mathcal{V}_{i0s}/\mathcal{V}_{i00}$, and $\mathcal{V}_{iss}/\mathcal{V}_{i00}$ used for each system are given in Table II. The solute and solvent hard core dimensions are—with very minor deviations-the estimates of Martire et al.,[4] based on tabulated Van der Waals volumes.[5] The procedure used to evaluate the ratios of ϵ's and $\mathcal{V}_i$'s was as follows. First, a value of $\mathcal{V}_{iss}/\mathcal{V}_{i00}$ was selected using the rough approximation

$$\frac{\mathcal{V}_{iss}}{\mathcal{V}_{i00}} \approx \frac{\Delta H_{\text{vap},s}/\rho_s}{\Delta H_{\text{vap},0}/\rho_0} , \qquad (26)$$

together with literature values for heats of vaporization and densities for the solvent and solute. (For the former, the heats of vaporization had to be estimated.) $\epsilon_{ss}/\epsilon_{00}$ was then obtained from (22) and the relations

$$\frac{\epsilon_{00}}{\mathcal{V}_{i00}a^3} = \begin{Bmatrix} 5.9 \\ 6.7 \end{Bmatrix} \quad \text{when } x = \begin{Bmatrix} 3.0 \\ 4.2 \end{Bmatrix} , \qquad (27)$$

derived from the results of Gelbart and Gelbart.[2] Finally, ϵ_{0s} was set equal to the geometric mean of ϵ_{00} and ϵ_{ss} (for lack of a better idea) and $\mathcal{V}'_{i0s}/\mathcal{V}_{i00}$ calculated using (21). Two different procedures were used to obtain $\epsilon_{00}, \mathcal{V}_{i00}$, and $\mathcal{V}_{a00}$. In

the first, $\mathcal{V}_{a00}/\mathcal{V}_{i00}$ was set equal to the value calculated by Gelbart and Gelbart using (12); namely, 0.25 when $x_0 = 3.0$ (MBBA) and 0.20 when $x_0 = 4.2$ (DHAB); in the alternative procedure, considerably smaller values of $\mathcal{V}_{a00}/\mathcal{V}_{i00}$: 0.080 for MBBA and 0 085 for DHAB, were used. In either case, $\mathcal{V}_{i00}$ was then chosen to give roughly the correct $N \rightarrow I$ transition temperature for the pure solvent[6] and ϵ_{00} was determined from (27). Both sets of parameters $\mathcal{V}_{i00}$, $\mathcal{V}_{a00}$, and ϵ_{00} are given in Table III, together with the values of $T_{N \rightarrow I}, \Delta S_{N \rightarrow I}, \Delta \rho/\rho_{\text{nem}}$, and $\eta_0(\rho_{\text{nem}})$ for the pure solvent which result from their use. The second procedure was designed to compensate, in part, for one of the major defects of the Van der Waals approach, its substantial overestimate of the quantitiy $N^{-1}E_{c,\text{nem}}(\rho, T)$ $-N^{-1}E_{c,\text{iso}}(\rho, T)$. This difficulty, presumably caused in large part by the failure to take into account short-range orientational correlations when evaluating the mean-field potential $\bar{\psi}_0$, results in unrealistically large values of the nematic order parameter and the discontinuities in density, entropy, and enthalpy at the $N \rightarrow I$ transition. As is clear from the table, much better (though still far from quantitatively satisfactory) results for $\eta_0, \Delta S_{N \rightarrow I}, \Delta \rho_{N \rightarrow I}/\rho_{\text{nem}}$, etc. are obtained using smaller values of $\mathcal{V}_{a00}/\mathcal{V}_{i00}$. ($\mathcal{V}_{a00}/\mathcal{V}_{i00} = 0.080$ and 0.085 were chosen, rather than still smaller ratios, because ratios slightly less than 0.10 are believed to explain the density dependence of the order parameter η best.[7]) We utilized the second procedure in most of our computations. In order to determine the effects of changes in $\mathcal{V}_{a00}/\mathcal{V}_{i00}$,

TABLE III. The two sets of solvent parameters (ϵ_{00}, $\mathcal{V}_{i00}$, $\mathcal{V}_{a00}$) used in the calculations, together with the resulting values of the temperature $T_{N \rightarrow I}$, order parameter η_0^{trans}, entropy change $\Delta S_{N \rightarrow I}$, and relative density discontinuity $\Delta \rho_{N \rightarrow I}/\rho_{\text{nem}}$ at the nematic $\rightarrow$ isotropic transition of the pure solvent.

Solvent	$\dfrac{\mathcal{V}_{a00}}{\mathcal{V}_{i00}}$	$\dfrac{\mathcal{V}_{i00}}{v_0 k_B}$ (K)	$\dfrac{\epsilon_{00}}{a^6 k_B}$ (K)	$T_{N \rightarrow I}$	η_0^{trans}	$\dfrac{\Delta S_{NI}}{N k_B}$	$\dfrac{\Delta \rho_{N \rightarrow I}}{\rho_{\text{nem}}}$
MBBA	0.080	2.00×10^4	2.0×10^6	328	0.542	0.887	0.041
MBBA	0.25	1.26×10^4	1.2×10^6	328	0.642	1.75	0.143
DHAB	0.085	2.20×10^4	3.6×10^6	405	0.621	1.32	0.090
DHAB	0.20	1.70×10^4	2.8×10^6	405	0.694	2.15	0.195

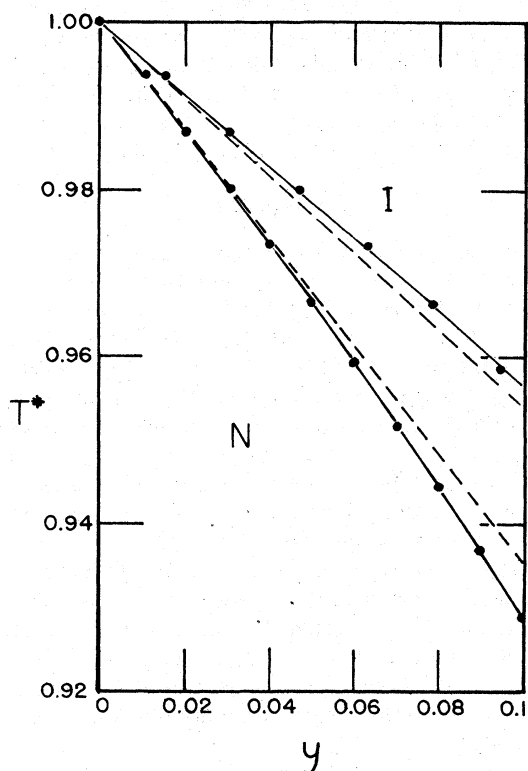FIG. 2. Predicted and observed phase diagrams for the system $(CH_3)_4Sn$-MBBA. The points were obtained by solving (16) and (23), using $a = 2.5$ Å, $x_0 = 3.0$, $R_a = 1.25$, and the set of energy parameters based on $\mathcal{V}_{a\,00} = 0.080\mathcal{V}_{i00}$. The dashed lines were constructed from the data of Martire et al. (Ref. 4). T^* and y are defined in Fig. 1.

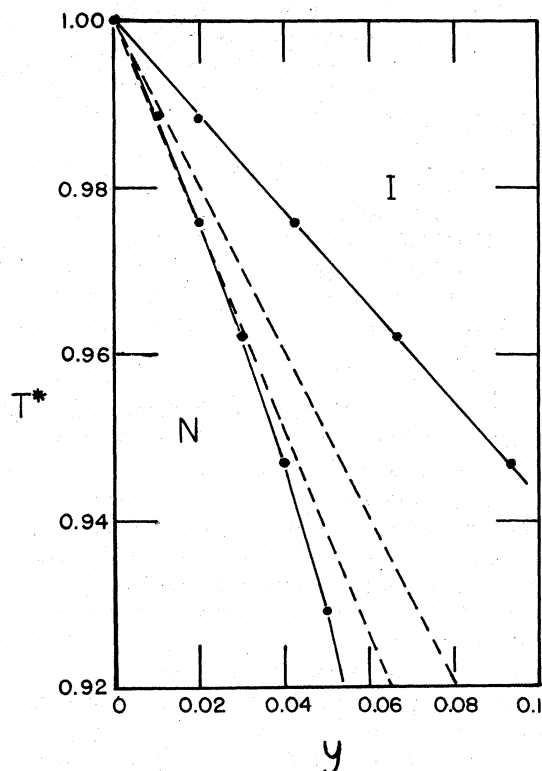FIG. 3. Predicted and observed phase diagrams for the system $(C_3H_7)Sn$-MBBA. The points were obtained by solving (16) and (23), using $a = 2.5$ Å, $x_0 = 3.0$, $R_a = 1.57$, and the set of energy parameters based on $\mathcal{V}_{a00} = 0.08\mathcal{V}_{i00}$. The dashed lines were constructed from the data of Martire et al. (Ref. 4). T^* and y are defined in Fig. 1.

however, the limiting slopes, β_n^∞ and β_i^∞, of the nematic and isotropic phase boundary lines were also calculated using the first procedure.

Reduced temperature $(T^* = T/T_{N\to I}^0)$ versus solute mole fraction phase diagrams were calculated for all six binary systems. Two of them, corresponding to the systems $(CH_3)_4SN$-MBBA and $(C_3H_7)_4Sn$-MBBA are presented in Figs. 2 and 3, respectively. For comparison, phase boundaries construct-

ed from the data of Martire et al.[4] are also shown (dashed lines). As can be seen, the predicted and observed nematic phase boundaries are in quite satisfactory agreement. However, the predicted two phase regions are wider than the observed ones and the discrepancy increases with increasing solute size. Similar conclusions can be drawn from Table IV, where experimental and theoretical values of the limiting slopes β_n^∞ and β_i^∞ are

TABLE IV. Theoretical and experimental values of the limiting slopes, β_n^∞ and β_i^∞, of the nematic and isotropic phase boundaries as $y \to 0$.

System	Experimental slopes		Theoretical slopes	
	β_n^∞	β_i^∞	β_n^∞	β_i^∞
CCl_4 − DHAB	−0.276	−0.255	−0.226	−0.174
$(CH_3)_4Sn$ − MBBA	−0.64	−0.46	−0.647	−0.411
$(C_2H_5)_4Sn$ − MBBA	−0.93	−0.84	−0.808	−0.471
$(C_3H_7)_4Sn$ − MBBA	−1.23	−0.99	−1.129	−0.564
$(C_3H_9)_4Sn$ − MBBA	−1.53	−1.25	−1.593	−0.660

TABLE V. Calculated limiting slopes, β_n^∞ and β_i^∞, of the nematic and isotropic phase boundaries obtained using $\mathcal{V}_{i00} = 1.26 \times 10^4$ K and $\mathcal{V}_{a00} = 0.25\mathcal{V}_{i00}$ for MBBA and $\mathcal{V}_{i00} = 1.70 \times 10^4$ K and $\mathcal{V}_{a00} = 0.20\mathcal{V}_{i00}$ for DHAB.

System	β_n^∞	β_i^∞
CCl_4 – DHAB	−0.267	−0.170
$(CH_3)_4$Sn – MBBA	−0.701	−0.315
$(C_2H_5)_4$Sn – MBBA	−0.830	−0.339
$(C_3H_7)_4$Sn – MBBA	−1.164	−0.384
$(C_4H_9)_4$Sn – MBBA	−1.719	−0.429

compared for all the systems studied. The large predicted values of $y_{iso} - y_{nem}$ clearly have the same origin as the large values of η_0, $\Delta S_{N \to I}$, and $\Delta\rho/\rho_{nem}$ seen in Table III. As noted above, one important factor contributing to these large discontinuities is the neglect of short-range orientational correlations other than hard rod exclusions. Such correlations are present in both the nematic and isotropic phases of real nematogens; as a result, the thermodynamic properties of a nematic mesophase are considerably more similar to those of the corresponding isotropic liquid at the same T and P than is predicted by the theory.

The calculations on which Figs. 2 and 3 and Table IV are based were all performed using $\mathcal{V}_{a00}$ = 0.080 $\mathcal{V}_{i00}$ for MBBA and $\mathcal{V}_{a00} = 0.085$ $\mathcal{V}_{i00}$ for DHAB. The limiting slopes obtained using $\mathcal{V}_{a00}$ = 0.25 $\mathcal{V}_{i00}$ for MBBA and $\mathcal{V}_{a00} = 0.20$ $\mathcal{V}_{i00}$ for DHAB

are presented in Table V. Although the values of β_i^∞ are considerably worse than the theoretical values in Table IV, it is gratifying to note that the two sets of β_n^∞'s are quite similar. Hence, it appears that very reasonable values of β_n^∞ are obtained no matter what ratios $\mathcal{V}_{a00}/\mathcal{V}_{i00}$ are used.

III. CONCLUSIONS

Although our Van der Waals theory suffers from the usual defects of calculations which neglect short range orientational order, we are able to predict quite satisfactorily the nematic phase boundary lines for all the binary solutions studied, using very reasonable *a priori* estimates of the effective solvent and solute hard-core dimensions and of the relative strengths of solvent-solvent and solute-solute attractions. This agreement strongly suggests that in the real nematogenic systems considered, as well as in the model systems, the limit of stability of the nematic order and the onset of phase separation are controlled primarily by excluded volume effects and the overall strength of the intermolecular attractions, while the orientation-dependence of the solvent-solvent attractions plays a relatively minor role at best.

[1]M. A. Cotter and D. C. Wacker, preceding paper, Phys. Rev. A 18, 2669 (1978).

[2]W. M. Gelbart and A. Gelbart, Mol. Phys. 33, 1387 (1977).

[3]M. A. Cotter (unpublished).

[4]D. E. Martire, G. A. Oweimreen, G. I. Ågren, S. G. Ryan, and H. T. Peterson, J. Chem. Phys. 64, 1456 (1976).

[5]A. Bondi, J. Phys. Chem. 68, 441 (1964).

[6]Because of the expense of the computations, we did not try to fit the transition temperatures to better than ±10 K. In any event, small changes in $T_{N \to I}^0$ have a negligible effect on the reduced temperature vs mole fraction phase diagrams or on such quantities as $\Delta S_{N \to I}$, η_0, $\Delta \rho_{N \to I}$, etc.

[7]See, for example, M. A. Cotter, J. Chem. Phys. 66, 1098 (1977).